JTCM Journal of Traditional Chinese Medicine

Online Submissions: http://www.journaltcm.com
ISSN 0255-2922
info@journaltcm.com

Original Article

Efficacy of Sailuotong (塞络通) on neurovascular unit in amyloid precursor protein/presenilin-1 transgenic mice with Alzheimer's disease

SUN Linjuan, LI Chengfu, LIU Jiangang, LI Nannan, HAN Fuhua, QIAO Dandan, TAO Zhuang, ZHAN Min, CHEN Wenjie, ZHANG Xiaohui, TONG Chenguang, CHEN Dong, Qi Jiangxia, LIU Yang, LIANG Xiao, ZHENG Xiaoying, ZHANG Yunling

SUN Linjuan, LIU Jiangang, LI Nannan, QIAO Dandan, ZHAN Min, CHEN Wenjie, ZHANG Xiaohui, TONG Chenguang, CHEN Dong, Qi Jiangxia, LIU Yang, LIANG Xiao, ZHANG Yunling, Department of Neurology, Xiyuan Hospital, China Academy of Chinese Medical Sciences, Beijing 100091, China
LI Chengfu, China Population and Development Research Center, Beijing 100081, China
ZHENG Xiaoying, Department of Institute of Population Research, Peking University, Beijing 100087, China
TAO Zhuang, Graduate School of China Academy of Chinese Medical Sciences, Beijing 100700, China
HAN Fuhua, Graduate School of Beijing University of Chinese Medicine, Beijing 100029, China
Supported by National Natural Science Foundation of China (81503450): Experimental study on the treatment of transgenic mice with Alzheimer's disease by protecting neurovascular unit by supplementing *Qi* and activating blood circulation investigate
Correspondence to: ZHANG Yunling, Department of Neurology, Xiyuan Hospital, China Academy of Chinese Medical Sciences, Beijing 100091, China. ling_zhangyun@yeah.net; **ZHENG Xiaoying,** Department of Institute of Population Research, Peking University, Beijing 100087, China. zhengxiaoying@sph.pumc.edu.cn
Telephone: +86-13910764257
DOI: 10.19852/j.cnki.jtcm.20240203.007
Received: December 22, 2022
Accepted: April 8, 2023
Available online: March 5, 2024

Abstract

OBJECTIVE: To discuss the influence of Sailuotong (塞络通, SLT) on the Neurovascular Unit (NVUs) of amyloid precursor protein (APP)/presenilin-1(PS1) mice and evaluate the role of gas supplementation in activating blood circulation during the progression of Alzheimer's disease (AD).

METHODS: The mice were allocated into the following nine groups: (a) the C57 Black (C57BL) sham-operated group (control group), (b) ischaemic treatment in C57BL mice (the C57 ischaemic group), (c) the APP/PS1 sham surgery group (APP/PS1 model group), (d) ischaemic treatment in APP/PS1 mice (APP/PS1 ischaemic group), (e) C57BL mice treated with aspirin following ischaemic treatment (C57BL ischaemic + aspirin group), (f) C57BL mice treated with SLT following ischaemic treatment (C57BL ischaemic + SLT group), (g) APP/PS1 mice treated with SLT (APP/PS1 + SLT group), (h) APP/PS1 mice treated with donepezil hydrochloride following ischaemic treatment (APP/PS1 ischaemic + donepezil hydrochloride group) and (i) APP/PS1 mice treated with SLT following ischaemic treatment (APP/PS1 ischaemic + SLT group). The ischaemic model was established by operating on the bilateral common carotid arteries and creating a microembolism. The Morris water maze and step-down tests were used to detect the spatial behaviour and memory ability of mice. The hippocampus of each mouse was observed by haematoxylin and eosin (HE) and Congo red staining. The ultrastructure of NVUs in each group was observed by electron microscopy, and various biochemical indicators were detected by enzyme-linked immunosorbent assay (ELISA). The protein expression level was detected by Western blot. The mRNA expression was detected by quantitative real-time polymerase chain reaction (qRT-PCR).

RESULTS: The results of the Morris water maze and step-down tests showed that ischemia reduced learning and memory in the mice, which were restored by SLT. The results of HE staining showed that SLT restored the pathological changes of the NVUs. The Congo red staining results revealed that SLT also improved the scattered orange–red sediments in the upper cortex and hippocampus of the APP/PS1 and APP/PS1 ischaemic mice. Furthermore, SLT significantly reduced the content of Aβ, improved the vascular endothelium and repaired the mitochondrial structures. The ELISA detection, western blot detection and qRT-PCR showed that SLT significantly increased the vascular endothelial growth factor (VEGF), angiopoietin and basic fibroblast growth factor, as well as the levels of gene and protein expression of low-density lipoprotein receptor-related protein-1 (LRP-1) and VEGF in brain tissue.

CONCLUSIONS: By increasing the expression of VEGF, SLT can promote vascular proliferation, up-regulate the expression of LRP-1, promote the clearance of Aβ and improve the cognitive impairment of APP/PS1 mice.

These results confirm that SLT can improve AD by promoting vascular proliferation and Aβ clearance to protect the function of NVUs.

Keywords: Alzheimer disease; amyloid beta-protein precursor; presenilin-1; mice, transgenic; replenishing *Qi* and activating blood; neurovascular unit; Sailuotong

1. INTRODUCTION

Alzheimer's disease (AD) is the most common cause of dementia and accounts for up to 80% of all dementia diagnoses.[1] Although overall death rates from stroke and cardiovascular disease are declining in the United States, the proportion of AD-related deaths increased by 89% between 2000 and 2014.[2] In addition to the amyloid-beta (Aβ) plaques and neurofibrillary tangles that define AD, 60%-90% of AD brains had evidence of cerebrovascular disease.[3] Despite decades of promising research, there are currently no effective drugs for AD. This may be due in part to the complex interplay of amyloid and tau disorders, neuroinflammation and cerebrovascular damage, as well as the significant challenges in defining and staging AD.[4]

Currently, the pathogenesis of AD remains unclear. However, the following two main hypotheses have been proposed:[5] (a) the amyloid plaques are pathogenic, and (b) Oligomer intermediates (or the colloids of fibril formation) are pathogenic. Amyloid fibrils can further aggregate into a gel; there is a potential link between gelation and cellular death because gels are known to eliminate large amounts of flow at a macro level.[6] However, at the microscopic level, bulk flow under hydrostatic pressure remains an area of research. New methods need to be developed to determine whether amyloid plaques obstruct fluid flow and the circulation of nutrients, waste and bio-signalling molecules through brain tissues and extracellular spaces.[7]

Although the amyloid hypothesis is the most well developed, multiple reports have suggested a weak association between Aβ deposition and neuronal atrophy and cognitive impairment.[8] Neurovascular triad model challenges the traditional pathogenesis hypothesis of AD.[9] At the same time, this model also raises a series of important new issues that need further study. For example, little is known about the molecular basis of the neurovascular association with neurodegenerative diseases, the adhesion molecules that hold the physical connections of various cell types together, the molecular crosstalk between different cell types (including endothelial cells, pericytes and astrocytes) and how these cellular interactions affect neuronal activity.[10] Addressing these issues could create new opportunities to better understand the molecular basis of the neurovascular link with neurodegeneration and develop novel neurovascular-based medicines.

In most pathological reports of AD complicated with vascular lesions, 60%-90% of AD patients showed cerebrovascular lesions at autopsy. Changes in cerebral blood vessels and blood flow play a key role in AD and have been shown to decrease in patients diagnosed with AD. Evidence from AD animal models also suggests that cerebral ischemia plays an important role in the pathogenesis of AD. After focal ischemia due to middle cerebral artery occlusion, amyloid precursor protein (APP) overexpressing mice show larger infarct volumes than wild-type controls.

The neurovascular unit (NVU) includes brain endothelial cells, pericytes or vascular smooth muscle cells, glia and neurons.[11] The NVU controls blood-brain barrier (BBB) permeability and cerebral blood flow; it also maintains the chemical composition of the neuronal environment, which is necessary for the proper functioning of neuronal circuits. Recent evidence indicates that BBB dysfunction is related to the accumulation of several vasculotoxic and neurotoxic molecules within the brain parenchyma, decreased cerebral blood flow and hypoxia. Together, these vascular-derived issues might initiate or contribute to neuronal degeneration.[10] This article examines the mechanisms of BBB dysfunction in AD and highlights therapeutic opportunities relating to these neurovascular deficits.

Traditional Chinese medicine (TCM) is a unique and complex medical system. After thousands of years of development, it is widely used in vascular ischemia treatment in Asia as a supplementary therapy of Western Medicine. The combination of TCM and Western Medicine has demonstrated good effects in relieving symptoms, promoting neurological function recovery and improving the quality of life of patients with ischemia.[12,13]

The theory of *Qi* and blood circulation is one of the basic theories of TCM. *Qi* describes the nutrients that constitute a human body and maintains life activities, so it is closely related to blood.[14] While TCM also uses blood to describe the functions of the body, in most cases, it is considered the same as blood in Western Medicine. Hence, supplementing *Qi* is another form of activating blood circulation.

Sailuotong (塞络通, SLT) is a new standardised TCM treatment composed of key bioactive components in concentrated extracts of Renshen (*Radix Ginseng*), Yinxingye (*Folium Ginkgo*) and Honghua (*Flos Carthami*) and has been proven to promote blood circulation and tonify *Qi* on ischaemic brain injuries. The clinically recommended dose of SLT is 180 mg/d for a patient weighing 70 kg, and the recommended dose in mice is 32 mg • kg^{-1} • d^{-1} based on the dose conversion per unit of body weight.[15]

This study investigates the changes of NVUs in amyloid precursor protein (APP)/presenilin-1(PS1) mice after SLT tonify *Qi* and activating blood circulation and discusses the role of tonify *Qi* and activating blood circulation in AD progression.

2. MATERIALS AND METHODS

2.1. Animal experiments

Six-week-old C57BL/6 and APP/PS1 mice were

purchased from Beijing Huafukang Biotechnology, Beijing, China. Up to five mice were in a ventilated cage at a time with a 12-h light/dark cycle and free access to food and water.

2.2. Ischaemic model

The ischaemic model was established by operating on the bilateral common carotid artery to create a microembolism. The mice were intraperitoneally anesthetised with pentobarbital at 3.5% chloral hydrate (0.1 mL/10 g body weight). A midline ventral incision was made in the neck. Both right and left common carotid arteries were separated, and the arterial blood vessel was stimulated with a temperature-controlled current of 80 mu A using an *in vivo* thrombometer (BT 87-3, Kunlun Institute of Biochemical Application Technology Development, Baotou, China) to cause thrombosis. The temperature sensor detected changes in the surface temperature of the blood vessels, and when the temperature in the distal part of the blood vessels dropped suddenly, blood vessel thrombosis occurred. All animals received a post-operative injection of penicillin (20 000 i.u. kg^{-1}; i.m.) to prevent infection.[16] Mice that survived 24 h after surgery were included in the experiment.

2.3. Experimental design

The animals were randomly grouped. Each group had 20 mice, 10 males and 10 females. The animal groupings were as follows: (a) the C57BL sham-operated group (control group), (b) ischaemic treatment in C57BL mice (C57 ischaemic group), (c) the APP/PS1 sham surgery group (APP/PS1 model group), (d) ischaemic treatment in APP/PS1 mice (APP/PS1 ischaemic group), (e) C57BL mice treated with aspirin following ischaemic treatment (C57BL ischaemic + aspirin group), C57BL mice treated with SLT following ischaemic treatment (C57BL ischaemic + SLT group), (g) APP/PS1 mice treated with SLT (APP/PS1 + SLT group), (h) APP/PS1 mice treated with donepezil hydrochloride following ischaemic treatment (APP/PS1 ischaemic + donepezil hydrochloride group) and (i) APP/PS1 mice treated with SLT following ischaemic treatment (APP/PS1 ischaemic + SLT group). The APP/PS1 ischaemic + donepezil hydrochloride group were administered intragastrically with 20 $mg \cdot kg^{-1} \cdot d^{-1}$ of donepezil hydrochloride.[17] The C57BL ischaemic + aspirin group were administered intragastrically with 32 $mg \cdot kg^{-1} \cdot d^{-1}$ of aspirin, the SLT group were administered intragastrically with 32 $mg \cdot kg^{-1} \cdot d^{-1}$ of SLT and the control group were given 32 $mg \cdot kg^{-1} \cdot d^{-1}$ of solvent. This study was performed in strict compliance with the local guidelines for the care and use of laboratory animals while respecting the policies on the use of animals in neuroscience research released by the American Society of Neuroscience. This study was conducted in accordance with the Declaration of Helsinki and approved by the ethics committee of Xiyuan Hospital (Approval No. 2018XLC012-2). All animal ethics requirements were strictly observed during the animal experiments. Surgery was performed under appropriate sedation, analgesia or anaesthesia, and every effort was made to minimise the distress and suffering of the animals.

2.4. Reagents and instruments

The following instruments were used: a Morris water maze test (Beijing Zhongshi Dichuang Technology Development Co., Ltd., Beijing, China), a step-down test (Beijing Zhongshi Dichuang Technology Development Co., Ltd., Beijing, China), an immunohistochemical staining results image analysis instrument (DpxView Pro computer colour image processing system, Copenhagen, Denmark) and a transmission electron microscope (TEM) (H-7500, Hitachi, Japan). Aspirin was purchased from Aladdin (Shanghai, China, MFCD00002430), and donepezil hydrochloride was obtained from Aladdin (Shanghai, China, MFCD17215939) as the positive drug. The SLT capsule utilised (invention patent No. ZL02131435.7) was composed of Renshen (*Radix Ginseng*), Yinxingye (*Folium Ginkgo*), Honghua (*Flos Carthami*) and other Chinese medicinal materials. These capsules were prepared as follows. Ethanol was added into Renshen (*Radix Ginseng*), Yinxingye (*Folium Ginkgo*) and Honghua (*Flos Carthami*) and was reflux-extracted three times and filtered. The filtrate was passed through macroporous adsorption resin and eluted with a water and ethanol ladder. The ethanol eluate was collected, after which the ethanol was recovered and spray-dried to obtain the effective components (e.g. total saponins of ginsenoside, total ketoesters of Yinxingye (*Folium Ginkgo*) and total glycosides of Stigma Croci). The components were then encapsulated at 60 mg/granule. Each SLT capsule contained 22.9% of total ginsenoside, 33.8% of total ketoesters of Yinxingye (*Folium Ginkgo*) and 4.5% of total crocin. SLT capsules were produced on a pilot scale by Shenwei Pharmaceutical Group (Langfang, China) and identified and stored under batch number 090914.

2.5. Behavioural testing

The Morris water maze test consisted of a circular pool (120 cm in diameter and 50 cm in height). The pool was filled with water at a temperature of (20 ± 2) ℃ to a depth of 30 cm. The pool was divided into four quadrants, and the platform was placed in the centre of one quadrant, with the location of this target quadrant counterbalanced across all the groups. The platform (diameter = 10 cm) was hidden 1.5 cm underneath the water's surface. The mice were tested in the quadrants using a fixed order, and an identical order of starting positions was used for all mice. For the hidden platform training, the mice were given training of four trials each day for five consecutive days. During training, the mice were placed into the water from a fixed position in each quadrant. The mice were placed into the water facing the wall. Each trial ended either after 180 s if the mouse did not find the

platform or 5 s after the mouse found the platform. The time needed for the mice to search for and climb the platform in the water was recorded within 3 min; this was regarded as the escape latency. If the mice did not find the platform within 3 min, the researcher guided them to the platform for 10 s, and the escape latency was recorded as 180 s. The probe trial (180 s), in which the platform was removed, was performed 24 h after the end of the fifth day of training. The camera system automatically recorded the number of times the mice entered and left the original platform area within 3 min and the swimming time and distance in the quadrant of the original platform as indicators to evaluate the learning and memory performance of the mice.[17]

The step-down apparatus consisted of a gridded floor box with a platform at the centre. During the training session, animals were placed on the platform, and the time for stepping down was recorded. Once the animals placed all their paws on the metallic grid, an electric shock of 0.8 mA was applied for 2 s. The test session took place 24 h after training when the animals were again placed on the platform and latency to step down from it was measured. Data are expressed as latencies to step down from the platform during training and test sessions or as a retention score (step-down latency in the training session subtracted from latency in the test session for each animal). [18]

2.6. Tissue preparation

Tissue blocks were processed for electron microscopy according to a method described in a previous study. For the light microscopy studies, the APP/PS1 and wild-type C57BL mice were anaesthetised with 10% chloral hydrate (0.004 mL/g) and transcardially perfused with 0.1 M phosphate-buffered saline (PBS), followed by 4% paraformaldehyde, 75-mM lysine and 10-mM sodium metaperiodate in 0.1-M phosphate buffer (PB). The fixed and cryoprotected brains were serially sectioned at a thickness of 40 μm in the coronal plane on a freezing microtome.[19] For the Western blot analysis and quantitative real-time polymerase chain reaction (qRT-PCR), unfixed and frozen mouse hippocampi samples were used. The mice were anaesthetised and transcardially perfused with cold saline, followed by 0.1 M of PBS containing 4% PFA and 4% glutaraldehyde. The brains were removed, and 1-mm3 samples were taken from the brain and examined with an electron microscope[20] (JEOL JEM 1400, JEOL, Beijing, China). The microvessels were observed using ink–gelatine perfusion. The coronal tissue was cut into 30-μm-thick continuous frozen sections; the sections were selected from every five pieces and collected using the patch method with natural air drying. Congo red staining was used to observe the amyloidosis of the hippocampus and cortex in three sections of the CA1 region of the hippocampus at the same location.[21]

2.7. Immunohistochemical staining

The 5 μm brain slices were dewaxed, rehydrated and incubated in 3% H_2O_2 (w/v) for 10 min and 0.3% triton X-100 in PBS at room temperature for 10 min. Then the antigens in slices were retrieved with a tris-ethylene diamine tetraacetic acid repair solution and blocked with 5% bovine serum albumin. Mouse brain sections were incubated with primary antibodies [anti-$A\beta_{1-42}$ antibodies (Abcam, Cambridge, UK, ab201060, diluted 1∶500), anti-APP antibodies (Abcam, Cambridge, UK, ab32136, diluted 1∶300)] at 4 ℃ overnight. Finally, the stains were visualised with secondary antibodies. Images were acquired using an Olympus fluorescence microscope (Olympus Corporation, Tokyo, Japan). The same image acquisition settings were used for each staining.

2.8. Enzyme-linked immunosorbent assay analysis of amyloid-beta peptides, vascular endothelial growth factor, angiopoietin 1/2/3/4 and basic fibroblast growth factor expression in the hippocampus and cerebrospinal fluid

The samples were weighed and homogenised in an 8 × volume of PBS with a 4-(2-Aminoethyl) benzenesulfonyl fluoride hydrochloride protease inhibitor cocktail set (Cat #539131; Calbiochem, La Jolla, CA, USA). The soluble fraction was separated by centrifuging it at 4000 × *g* for 10 min. The pellets containing insoluble Aβ peptides were solubilised in a 5-M guanidine HCl/50-mM Tris HCl solution by incubating for 3.5 h on an orbital shaker at room temperature to obtain an insoluble fraction.[24] The method of collecting the cerebrospinal fluid of the mice was modified, and around 100-200 μL of the fluid was slowly extracted. The Content of the $A\beta_{1-42}$, vascular endothelial growth factor (VEGF), angiopoietin (Ang) (Ang1/2/3/4) and basic fibroblast growth factor (bFGF) were determined using commercially available human enzyme-linked immunosorbent assay (ELISA) kits (Cats #KHB3481 and #KHB3441; Invitrogen, Camarillo, CA, USA). Analysis of optical density was performed at 450 nm with a microplate reader.

2.9. Transmission electron microscopy

A transcardiac perfusion with 0.9% saline was performed to remove circulating blood; next, perfusion was conducted with a fixative containing 2% paraformaldehyde and 2.5% glutaraldehyde in 0.1-M PB (pH 7.4). The brains were dissected and postfixed in fresh fixative for 24 h at 4°C. Coronal sections (100 μm thick) were cut on a Leica VT1000 vibrating blade vibratome, and in the coronal section of interest, the subiculum of the hippocampal formation (termed hippocampus) was micro-dissected. The samples were washed in a cacodylate buffer containing 2-mM calcium chloride and postfixed for 1 h with reduced osmium (OsO_4 1% and $K_4Fe[CN]_6$ 1.5%); then, they were incubated in 1% tannic acid in a 0.1-M cacodylate buffer for 1 h before a final overnight incubation with 1% uranyl acetate in water.[20] The samples were dehydrated at room temperature with different grades of ethanol

(from 20% to 100%) for 5 min each, infiltrated with low-viscosity resin (TAAB Laboratories Equipment, Berkshire, UK) and polymerised for 24 h at 60 ℃. Last, ultrathin sections (70 nm) were cut using a Reichert-Jung Ultracut E ultramicrotome (Reichert Technologies Life Sciences, Buffalo, NY, USA), mounted on Athene 200-mesh thin-bar copper grids (Agar Scientific, UK) and visualised with a Tecnai 12 BioTwin TEM (FEI, Hillsboro, OR, USA) using a Gatan Orius SC1000 camera (Gatan, Pleasanton, IN, USA).

2.10. Western blot analysis for detecting vascular endothelial growth factor receptor for advanced glycation endproducts, lipoprotein receptor-related protein-1, α7-nicotinic acetylcholine receptor and Amyloid Beta 42 expression in brain tissue

Aliquots of the hippocampus homogenate containing 15 mg of protein per sample were analysed using the western blot method. The samples were placed in a sample buffer (0.5-m Tris–HCl, pH 6.8, 10% glycerol, 2% [w/v] Sodium dodecyl sulfate, 5% [v/v] 2-mercaptoethanol, 0.05% bromophenol blue) and denatured by boiling at 95-100 ℃ for 5 min. The samples were separated by electrophoresis on 10%-15% acrylamide gels. Next, the proteins were transferred to polyvinylidene fluoride membranes using a transblot apparatus. The membranes were blocked for 2 h with 5% non-fat milk dissolved in a tris buffered saline (TBS-T) buffer (50-mM Tris; 1.5% NaCl, 0.05% Tween 20, pH 7.5).[24] Then, they were incubated with primary antibodies: anti-Vessel Experience Factor on Discharging (VEDF) antibody (Abcam, Cambridge, UK) (ab32152) (diluted 1:500), anti-receptor for advanced glycation endproducts (RAGE) antibody (Abcam, Cambridge, UK) (ab216329) (diluted 1:500), anti-lipoprotein receptor-related-protein-1 (LRP-1) antibody (Abcam, Cambridge, UK) (ab92544) (diluted 1:20 000), anti-α7-nicotinic acetylcholine receptor (α7-nAChRs) antibody (Abcam, Cambridge, UK) (ab216485) (diluted 1∶300) and anti-$A\beta_{1-42}$ antibody (Abcam, Cambridge, UK) (ab201060) (diluted 1∶500). After overnight incubation, the blots were washed thoroughly in a TBS-T buffer and incubated for 1 h with a peroxidase-conjugated ImmunoglobulinG secondary antibody (1/2000).

Immunoreactive proteins were detected using a chemiluminescence-based detection kit [Immobilon Western Chemiluminescent HRP substrate (Merck) (42029053) (Shanghai Ease-Bio Technology Co., Ltd., Shanghai, China)]. Protein levels were determined by densitometry using a Chemidoc XRS + Molecular Imager detection system (Bio-Rad, Shanghai, China) and Image Lab image analysis software (Bio-Rad, Shanghai, China). Measurements were expressed as arbitrary units.

2.11. Real-time polymerase chain reaction analysis

A MiniBEST Universal RNA Extraction Kit (TaKaRa, Dalian, China) was used to extract the total RNA according to the manufacturer's guidelines. The RNA isolates were determined by 260/280-nm absorbance using a NanoDrop spectrophotometer (ND-1000, Thermo Fisher Scientific, Waltham, MA, USA). The RNA was reverse transcribed into cDNA using a PrimeScript™ RT reagent kit with a gDNA Eraser (TaKaRa, Osaka Prefecture, Japan), and the cDNA was quantified using SYBR® Premix Ex Taq™ II (TaKaRa, Osaka Prefecture, Japan). The reverse transcription system was 20 μL, and the conditions were 37 ℃ for 15 min and 85 ℃ for 5 s. After the reverse transcription, the cDNA was stored at –20 ℃ for reserve. A 2-μL cDNA template was taken and amplified in vitro according to the qRT-PCR reaction conditions, with a total volume of 25 μL. The amplification conditions were as follows: pre-denaturation for 30 s at 95 ℃, 5 s at 95 ℃ and 30 s at 60℃; 40 cycles of this were repeated. The relevant primers sequence are as follows: (a) The forward primers of VEGF: 5'-ATCATGCGGATCAAACCTCACC-3', the reverse primers: 5'-GGCTTTGTTCTGTCTTTC-TTTGGTC-3', the product size: 101 bp; (b) The forward primers of RAGE: 5'-GACGGGACTC-TTTACAC-TGCG-3', the reverse primers: 5'-CACCTTCAGGC-TCAACCAACA-3', the product size: 191 bp; (c) The forward primers of α7-nAChRs: 5'-CTGGCTTTG-CTGGTATTCTTG-3', the reverse primers: 5'-CACAATCACTGTCACGACCACT-3', the product size: 204 bp; (d) The forward primers of LPR1: 5'-TTCTGGTATAAGCGGCGAGTC-3'; the reverse primers: 5'-TCAGGGTCAAGGGCAAAATC-3', the product size:167 bp; (e) The forward primers of APP: 5'-TGGTGGACCCCAAGAAAGC-3', the reverse primers: 5'-GCCAAGACATCGTCGGAGTAG-3', the product size: 184 bp; (f) The forward primers of ACTIN: 5'-CGTTGACATCCGTAAAGACCTC-3', the reverse primers: 5'-ACAGAGTACTTGCGCTCAGGAG-3', the product size: 159 bp. Using β-actin as the internal control, the mRNA relative expression levels of each group were calculated according to the $2^{-\Delta\Delta Ct}$ algorithm.[25]

2.12. Statistical analysis

Data were statistically processed by SPSS Statistics 22 (IBM Corp., Armonk, NY, USA) and Origin 8.0 (OriginLab, Northampton City, MA, USA) and expressed as mean ± standard deviation. One-way analysis of variance was employed to make comparisons among groups, and in the case of the normal distribution, Tukey's post hoc test was conducted; otherwise, the Kruskal-Wallis test was adopted. Differences were regarded as significant with $P < 0.05$.

3. RESULTS

3.1. Influence of Sailuotong on the spatial learning and memory ability of mice

The Morris water maze test was used to detect the learning ability and memory function of mice in each group. The data in Table 1 is from the water maze test

(the space exploration experiment) conducted on the sixth day. The results shown in Table 1 compare the C57BL sham-operated group in terms of the number of crossings, swimming time and swimming distance with APP/PS1 model group ($P < 0.01$), APP/PS1 ischemia ($P < 0.01$) and C57BL ischemia ($P < 0.01$) groups; the values were significantly reduced, indicating that the mouse models were successful. Compared with the APP/PS1 model group, the number of crossings and the swimming distance in the APP/PS1 ischaemic group were clearly reduced ($P < 0.05$); the swimming time of the APP/PS1 ischaemic group was also significantly reduced ($P < 0.01$). Compared with C57BL ischemia group, the mice in C57BL ischaemic + aspirin group and C57BL ischaemic + SLT group had more crossings and longer swimming times ($P < 0.05$), indicating therapeutic effects. The swimming distance of C57BL ischaemic + SLT group increased significantly, which was statistically significant ($P < 0.01$). The number of crossings, swimming times and swimming distances of the mice in the APP/PS1 + SLT group ($P < 0.05$), APP/PS1 ischaemic + donepezil hydrochloride group ($P < 0.01$) and APP/PS1 ischaemic + SLT group ($P < 0.01$) significantly increased compared with APP/PS1 ischaemic group; these findings were statistically significant.

The results in Table 2 show that compared with the C57BL sham-operated group, the number of platform jumping errors in the C57BL ischemia ($P < 0.05$) and APP/PS1 ischemia ($P < 0.01$) groups were significantly increased. Compared with the C57BL sham-operated group, the incubation period of the C57BL ischemia ($P < 0.05$), the APP/PS1 model ($P < 0.01$) and the APP/PS1 ischemia ($P < 0.01$) groups were significantly shorter, with reduced memory function. Compared with the C57BL ischaemic group, the platform jumping errors and the effect of a prolonged incubation period in C57BL ischaemic + SLT group were statistically different ($P < 0.05$). Compared with the APP/PS1 ischemia group, the platform jumping errors of APP/PS1 + SLT group, APP/PS1 ischaemic + donepezil hydrochloride group (all

Table 1 Effect of the method of replenishing *Qi* and activating blood on the spatial learning and memory ability of APP/PS1 double transgenic ischemic mice ($\bar{x} \pm s$)

Group	Dose ($mg \cdot kg^{-1} \cdot d^{-1}$)	*n*	Number of crossings	Swimming time (s)	Swimming distance (cm)
C57 sham-operated	-	16	7.1±1.3	46.9±12.2	318.3±89.2
C57 ischemia	-	16	5.2±1.3[a]	39.1±10.4[a]	252.1±101.4[a]
APP/PS1 model	-	16	4.2±2.1[a]	37.2± 9.9[a]	275.2±97.3[e]
APP/PS1 ischemia	-	16	3.4±1.7[a]	33.0±11.2[a]	237.2±98.3[e]
C57BL ischaemic + aspirin	32	16	6.1±1.7[b]	45.4±12.4[b]	198.3±124.8[b]
C57BL ischaemic + SLT	32	16	6.4±1.7[b]	43.3±13.4[b]	298.2±69.9[f]
APP/PS1 + SLT	32	16	5.7±2.1[c]	46.3±9.3[d]	305.3±89.5[d]
APP/PS1 ischaemic + donepezil hydrochloride	20	16	5.3±2.2[c]	45.5±11.3[c]	333.6±76.7[c]
APP/PS1 ischaemic + SLT	32	16	6.8±2.2[f]	44.2±8.0[f]	341.3±81.1[f]

Notes: ischaemic treatment: both right and left common carotid arteries were separated, and the arterial blood vessel was stimulated with a temperature-controlled current of 80 mu A using an *in vivo* thrombometer to cause thrombosis. The APP/PS1 ischaemic + donepezil hydrochloride group were administered intragastrically with 20 $mg \cdot kg^{-1} \cdot d^{-1}$ of donepezil hydrochloride. The C57BL ischaemic + aspirin group were administered intragastrically with 32 $mg \cdot kg^{-1} \cdot d^{-1}$ of aspirin, the SLT group were administered intragastrically with 32 $mg \cdot kg^{-1} \cdot d^{-1}$ of SLT and the control group were given 32 $mg \cdot kg^{-1} \cdot d^{-1}$ of solvent. Duration: two months. SLT: Sailuotong; APP: amyloid precursor protein; PS1: presenilin-1presenilin-1. One-way analysis of variance was employed to make comparisons among groups, and in the case of the normal distribution, Tukey's post hoc test was conducted; otherwise, the Kruskal-Wallis test was adopted. Compared with C57 sham-operated group, [a]$P < 0.01$, [e]$P < 0.05$; compared with C57 ischemia group, [b]$P < 0.05$; [f]$P < 0.01$; compared with APP/PS1 ischemia group, [d]$P < 0.05$; [c] $P < 0.01$.

Table 2 Effect of the method of replenishing *Qi* and activating blood on step-down test of APP/PS1 double transgenic ischemic mice ($\bar{x} \pm s$)

Group	Dose ($mg \cdot kg^{-1} \cdot d^{-1}$)	*n*	Number of errors (times)	Incubation period (s)
C57 sham-operated	-	15	1.3±1.2	226.5±53.1
C57 ischemia	-	15	2.2±1.4[a]	179.2±55.3[a]
APP/PS1 model	-	14	2.6±1.3	167.7±61.2[a]
APP/PS1 ischemia	-	15	3.1±1.7[a]	156.8±54.9[a]
C57BL ischaemic + aspirin	32	15	1.3±1.3	217.5±64.4
C57BL ischaemic + SLT	32	15	1.2±1.5[b]	226.8±66.2[b]
APP/PS1 + SLT	32	14	1.5±1.1[c]	213.4±49.8[d]
APP/PS1 ischaemic + donepezil hydrochloride	20	15	1.5±1.6[c]	206.2±73.6[e]
APP/PS1 ischaemic + SLT	32	16	1.6±1.5[c]	239.5±62.5[e]

Notes: ischaemic treatment: both right and left common carotid arteries were separated, and the arterial blood vessel was stimulated with a temperature-controlled current of 80 mu A using an in vivo thrombometer to cause thrombosis. The APP/PS1 ischaemic + donepezil hydrochloride group were administered intragastrically with 20 $mg \cdot kg^{-1} \cdot d^{-1}$ of donepezil hydrochloride. The C57BL ischaemic + aspirin group were administered intragastrically with 32 $mg \cdot kg^{-1} \cdot d^{-1}$ of aspirin, the SLT group were administered intragastrically with 32 $mg \cdot kg^{-1} \cdot d^{-1}$ of SLT and the control group were given 32 $mg \cdot kg^{-1} \cdot d^{-1}$ of solvent. Duration: two months. SLT: Sailuotong; APP: amyloid precursor protein; PS1: presenilin-1presenilin-1.One-way analysis of variance was employed to make comparisons among groups, and in the case of the normal distribution, Tukey's post hoc test was conducted; otherwise, the Kruskal-Wallis test was adopted. Compared with C57 sham-operated group, [a]$P < 0.01$; compared with C57 ischemia group, [b]$P < 0.05$; [c]$P < 0.01$; compared with APP/PS1 ischemia group, [d]$P < 0.05$; [e]$P < 0.01$.

$P < 0.01$). Additionally, the incubation periods of APP/PS1 ischaemic + SLT group, APP/PS1 ischaemic + donepezil hydrochloride group and APP/PS1 ischaemic + SLT group were significantly longer ($P < 0.05$, $P < 0.01$ and $P < 0.01$, respectively).
These results indicate that SLT had a better impact on the spatial learning and memory ability of the mice with AD.

3.2. Pathological examination of each group

3.2.1. Haematoxylin and eosin (HE) staining to observe the pathological morphology

HE staining can reveal the general morphological and structural characteristics of various tissues or cells. The neurons in the CA1 region of the hippocampus of the C57BL sham-operated mice were uniformly stained, large in number, neat and densely arranged. Vacuolar degeneration and necrosis were rare. The CA1 region of the hippocampus of the mice in the C57BL ischemia group hardly changed. The number of neurons in the CA1 hippocampus region of the mice in the APP/PS1 model group was significantly reduced; some of the cell bodies had shrunk, the arrangement was disordered, the extracellular space was enlarged and the nuclear membrane was unclear. The APP/PS1 model ischemia group had fewer neurons in the CA1 hippocampus area; they were partly atrophied, parts of the cell bodies had shrunk, the extracellular spaces were enlarged and the cell structures were fuzzy, with more severe damage than in the APP/PS1 model group. In the SLT group, the number of neurons in the CA1 hippocampus area increased, the cell arrangement was restored to a certain extent, the cell structure was basically clear and the nuclear membrane was distinguishable; the cells occasionally exhibited vacuolar degeneration and nucleus pyknosis, and few cell necroses were observed (Figure 1A).

3.2.2 Congo red staining

The brain tissues of the mice in the C57BL sham-operated and C57BL ischemia groups were relatively clear, and no positive staining was observed. In the APP/PS1 model group, there were scattered orange-red sediments in the cerebral cortex and the upper margin of the hippocampus; these were mostly irregular-shaped, of different sizes and demonstrated uneven staining. Among them, the hippocampus was densely distributed. There was a certain increase in the red deposits in the cerebral cortex of the APP/PS1 ischemia model group, and scattered red sediments appeared in the upper margin and hippocampus. The cortex and hippocampus of APP/PS1 ischaemic + donepezil hydrochloride group also showed scattered orange-red staining, with more orange-red staining in the cortex; however, compared with the APP/PS1 ischemia model group, the staining was lighter, and the number was significantly reduced. Compared with the APP/PS1 ischaemic group, the positive staining in the SLT group was mainly limited to the cortex; the staining was lighter, and the number was significantly reduced (Figure 1B).
The results of the HE and Congo red staining revealed that SLT improved brain tissue in mice with AD.

3.3. Immunohistochemical detection of the hippocampus in each group

Figure 2A and Table 3 reveal that, compared with the C57BL sham-operated group, the APP/PS1 model and the APP/PS1 ischemia groups had an increase in the APP positive expression area ($P < 0.01$), which indicates that the mice models were successful. The APP/PS1 + SLT group, APP/PS1 ischaemic + donepezil hydrochloride group and APP/PS1 ischaemic + SLT group had a significant decrease in the APP positive expression area compared with the APP/PS1 ischaemic group ($P < 0.05$, $P < 0.01$ and $P < 0.01$, respectively).
Figure 2B and Table 3 show that, compared with the C57BL sham-operated group, the C57BL ischemia group, the APP/PS1 model group and the APP/PS1 ischemia group had an increased $A\beta_{1\text{-}42}$ positive expression ($P < 0.05$, $P < 0.05$ and $P < 0.01$, respectively), which indicates that the mouse models were successful. The C57BL ischaemic + SLT group group had a decreased $A\beta_{1\text{-}42}$ positive expression compared with the C57BL ischemia group ($P < 0.05$); the $A\beta_{1\text{-}42}$ positive expression areas of the APP/PS1 + SLT group, APP/PS1 ischaemic + donepezil hydrochloride group and APP/PS1 ischaemic + SLT group were lower than the APP/PS1 ischaemic group ($P < 0.05$, $P < 0.01$ and $P < 0.01$, respectively), and there was a statistically significant difference.

3.4. Enzyme-linked immunosorbent assay to detect the amyloid-beta content in the cerebrospinal fluid of each group

The results of ELISA showed that, compared with the C57BL sham-operated group, the APP/PS1 model and APP/PS1 ischemia groups had a slight decrease in cerebrospinal fluid Aβ content, which was a statistically significant difference ($P < 0.05$ and $P < 0.01$, respectively). Compared with the C57BL ischemia group, the Aβ content in the cerebrospinal fluid of the mice in the aspirin and SLT groups was not statistically different ($P > 0.05$). Compared with the APP/PS1 ischemia group, APP/PS1 ischaemic + donepezil hydrochloride group and APP/PS1 ischaemic + SLT group significantly reduced the elevated Aβ content in the cerebrospinal fluid, which was a statistically significant difference ($P < 0.01$) (Table 4).

3.5. Ultrastructure observation of the neurovascular units in each group

In the control group, the nuclear membrane was intact; the structure and quantity of chromatin were normal; the morphology and distribution of the mitochondria, endoplasmic reticulum, Golgi apparatus and nuclei were basically normal; and autophagosomes around the nucleus was rare. There were more mitochondrial

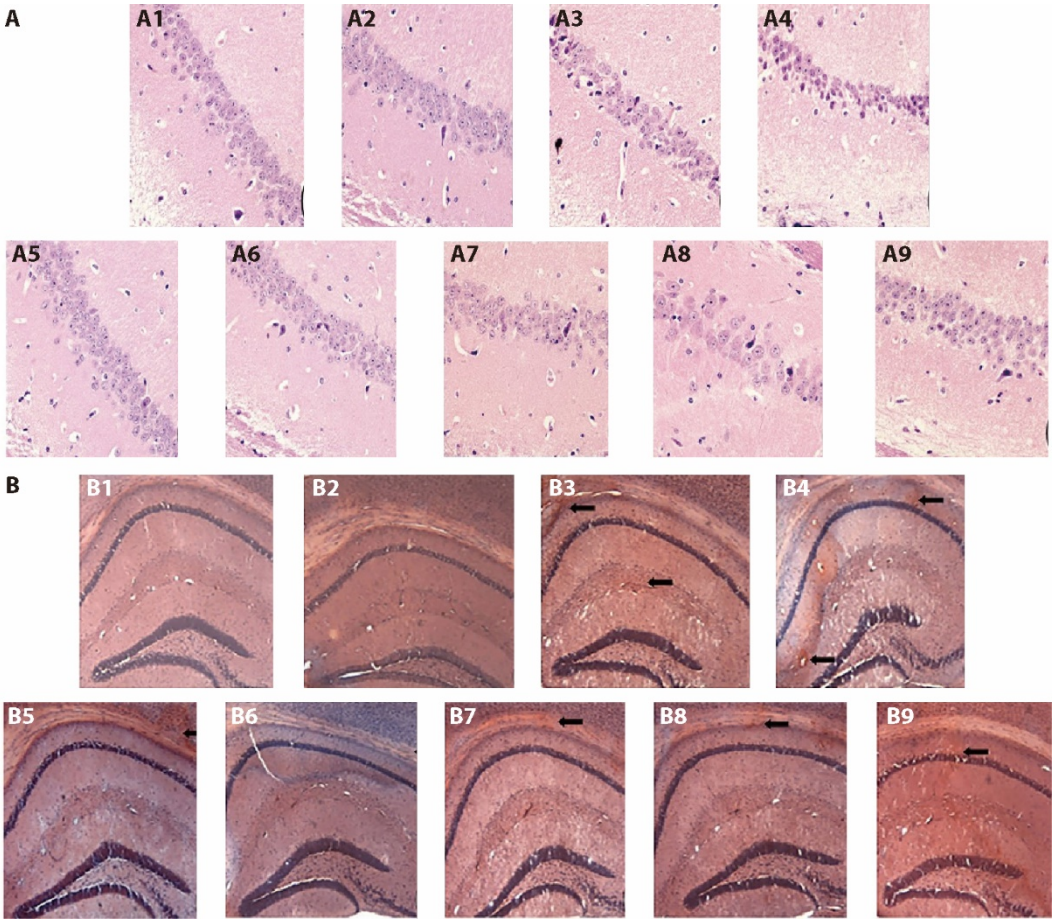

Figure 1 Effect of replenishing *Qi* and activating blood on pathological morphology and amyloid in the brain of APP/PS1 double transgenic ischemic mice

A: HE pathological staining × 400; B: Congo red staining × 40. A1/B1: C57 sham-operated group; A2/B2: C57 ischemia group; A3/B3: APP/PS1 model group; A4/B4: APP/PS1 ischemia group; A5/B5: C57BL ischaemic + aspirin group at dose of 20 mg·kg^{-1}·d^{-1} A6/B6: C57BL ischaemic + SLT group at dose of 32 mg·kg^{-1}·d^{-1}; A7/B7: APP/PS1 + SLT group at dose of 32 mg·kg^{-1}·d^{-1}; A8/B8: APP/PS1 ischaemic + donepezil hydrochloride group at dose of 32 mg·kg^{-1}·d^{-1}; A9/B9: APP/PS1 ischaemic + SLT group at dose of 32 mg·kg^{-1}·d^{-1}. Ischaemic treatment: both right and left common carotid arteries were separated, and the arterial blood vessel was stimulated with a temperature-controlled current of 80 mu A using an *in vivo* thrombometer to cause thrombosis. Duration: two months. SLT: Sailuotong; APP: amyloid precursor protein; PS1: presenilin-1presenilin-1.

vacuoles in the hippocampal neurons of the mice in the APP/PS1 group, and their structure was relatively intact. Mitochondrial vacuoles in the hippocampal neurons of the APP/PS1 ischaemic group increased significantly, and the vascular walls proliferated. In the APP/PS1 ischaemic group, the empty mitochondria in hippocampal nerve cells increased significantly, and the blood vessel walls proliferated (Figure 3A).

There were more empty mitochondria in the hippocampal nerve cells of the APP/PS1 mice, and their structure was relatively complete. The APP/PS1 ischaemic group had significantly more empty mitochondria in the hippocampal nerve cells, and the blood vessel walls proliferated. Compared with the APP/PS1 ischemia group, the SLT group had improved vascular endothelium and repaired mitochondrial structure (Figure 3B).

3.6. Enzyme-linked immunosorbent assay to detect the contents of the vascular endothelial growth factor, angiopoietin and basic fibroblast growth factor in each group

The results showed that, compared with the C57BL sham-operated group, the VEGF content of the C57BL ischemia group was significantly increased ($P > 0.01$). Compared with the C57BL ischemia group, the aspirin and SLT groups showed no statistical difference ($P > 0.05$). Compared with the APP/PS1 model group, the VEGF content of the mice in the APP/PS1 ischemia group increased. The use of SLT significantly increased the VEGF, Ang and bFGF content ($P < 0.05$). Compared with the APP/PS1 ischemia group, SLT significantly increased the content of Ang and bFGF in the APP/PS1 group ($P < 0.05$). The results are shown in Table 5.

3.7. Western blot to detect the expression of the vascular endothelial growth factor, Amyloid Beta 42, α7-nicotinic acetylcholine receptor, receptor for advanced glycation endproducts and lipoprotein receptor-related protein-1 proteins in the brain tissue of each group

The results showed that, compared with the C57BL sham-operated group, the expression of VEGF and α7-nAChRs in the brain tissue of the C57BL ischemia group increased to a certain extent ($P < 0.01$ and $P < 0.05$, respectively). The expression of $A\beta_{1-42}$, RAGE and LRP-

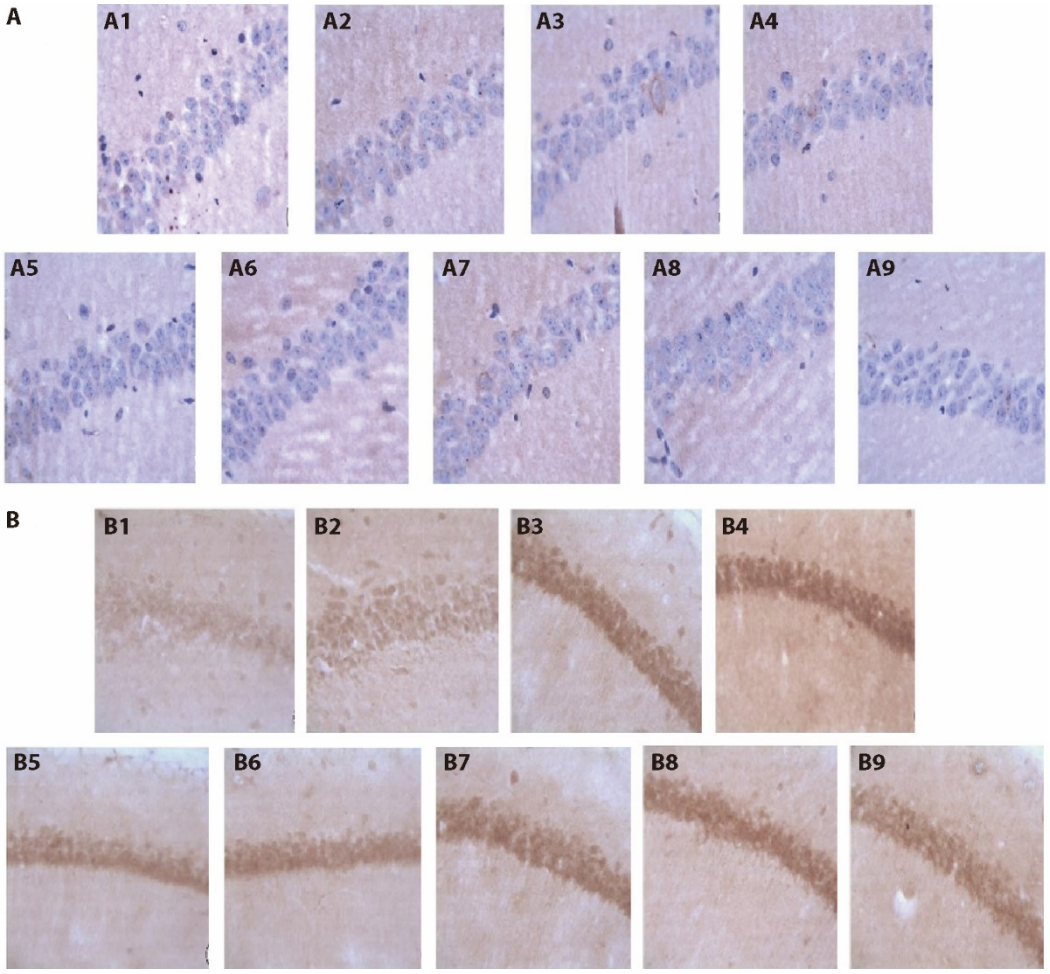

Figure 2 Effects of Invigorating *Qi* and Activating blood circulation on APP and $A\beta_{1-42}$ brain tissue of APP/PS1 double transgenic ischemic mice

A: APP positive expression × 400; B: $A\beta_{1-42}$ positive expression × 400. A1/B1: C57 sham-operated group; A2/B2: C57 ischemia group; A3/B3: APP/PS1 model group; A4/B4: APP/PS1 ischemia group; A5/B5: C57BL ischaemic + aspirin group at dose of 20 $mg \cdot kg^{-1} \cdot d^{-1}$ A6/B6: C57BL ischaemic + SLT group at dose of 32 $mg \cdot kg^{-1} \cdot d^{-1}$; A7/B7: APP/PS1 + SLT group at dose of 32 $mg \cdot kg^{-1} \cdot d^{-1}$; A8/B8: APP/PS1 ischaemic + donepezil hydrochloride group at dose of 32 $mg \cdot kg^{-1} \cdot d^{-1}$; A9/B9: APP/PS1 ischaemic + SLT group at dose of 32 $mg \cdot kg^{-1} \cdot d^{-1}$. Ischaemic treatment: both right and left common carotid arteries were separated, and the arterial blood vessel was stimulated with a temperature-controlled current of 80 mu A using an *in vivo* thrombometer to cause thrombosis. Duration: two months. SLT: Sailuotong; APP: amyloid precursor protein; PS1: presenilin-1presenilin-1.

1 in the C57BL ischemia group was relatively low, and there was no statistically significant difference. Compared with the C57BL sham-operated group, the expression of $A\beta_{1-42}$, α7-nAChRs and RAGE in the APP/PS1 model and APP/PS1 ischemia groups significantly increased to varying degrees (all $P < 0.05$). Compared with the C57BL ischemia group, the expression of VEGF was reduced ($P < 0.01$), and LRP-1 was increased in the C57BL ischemia aspirin group ($P < 0.05$). Compared with the APP/PS1 ischemia group, SLT significantly increased the expression of LRP-1 and VEGF and inhibited the expression of α7-nAChRs, RAGE and $A\beta_{1-42}$ in brain tissue ($P < 0.01$). The results are shown in Figure 4 and Table 6.

3.8. Quantitative real-time polymerase chain reaction to detect the expression of the vascular endothelial growth factor, amyloid precursor protein, α7-nicotinic acetylcholine receptor, receptor for advanced glycation endproducts and lipoprotein receptor-related protein-1 genes in the brain tissue of each group

The qRT-PCR results showed that, compared with the C57BL sham-operated group, the expression of the VEGF and LRP-1 genes in the brain tissue of the C57BL ischaemic group increased significantly ($P < 0.05$), and the C57BL ischaemic group had statistically lower gene expression levels of α7-nAChRs and RAGE ($P > 0.05$). Compared with the C57BL sham-operated group, the expression of the APP and RAGE genes increased, while the expression of the VEGF, α7-nAChRs and LRP-1 genes was reduced in the APP/PS1 model group and APP/PS1 ischemia group ($P < 0.05$). Compared with the C57BL ischaemic group, the expression of the VEGF, α7-nAChRs, RAGE and LRP-1 genes in C57BL ischaemic + aspirin group was reduced to varying statistically significant degrees ($P < 0.05$ and $P < 0.01$, respectively). Compared with the C57BL ischaemic group, the expression of the APP, α7-nAChRs, RAGE and LRP-1 genes was statistically significantly reduced in C57BL ischaemic + SLT group ($P < 0.05$ and $P < 0.01$, respectively). Compared with the APP/PS1 ischaemic group, SLT significantly increased the expression of the

Table 3 Effect of replenishing *Qi* and activating blood on APP and $A\beta_{1-42}$ expression in hippocampal CA1 region of APP/PS1 double transgenic ischemic mice ($\bar{x} \pm s$)

Group	Dose (mg/kg·d)	Visual field number (*n*)	APP	$A\beta_{1-42}$
C57 sham-operated	-	12	1.15±0.5	3.75±1.2
C57 ischemia	-	12	1.46±0.5	8.12±1.0[d]
APP/PS1 model	-	12	5.53±0.8[a]	19.12±5.2[d]
APP/PS1 ischemia	-	12	9.77±0.6[a]	31.43±9.2[a]
C57BL ischaemic + aspirin	32	12	1.28±0.4	7.18±3.2
C57BL ischaemic + SLT	32	12	1.14±0.5	5.12±4.4[e]
APP/PS1 + SLT	32	12	3.38±0.5[b]	14.38±5.4[b]
APP/PS1 ischaemic + donepezil hydrochloride	20	12	6.23±0.6[c]	16.24±6.4[c]
APP/PS1 ischaemic + SLT	32	12	7.18±0.4[c]	19.38±6.0[c]

Notes: ischaemic treatment: both right and left common carotid arteries were separated, and the arterial blood vessel was stimulated with a temperature-controlled current of 80 mu A using an *in vivo* thrombometer to cause thrombosis. The APP/PS1 ischaemic + donepezil hydrochloride group were administered intragastrically with 20 $mg \cdot kg^{-1} \cdot d^{-1}$ of donepezil hydrochloride. The C57BL ischaemic + aspirin group were administered intragastrically with 32 $mg \cdot kg^{-1} \cdot d^{-1}$ of aspirin, the SLT group were administered intragastrically with 32 $mg \cdot kg^{-1} \cdot d^{-1}$ of SLT and the control group were given 32 $mg \cdot kg^{-1} \cdot d^{-1}$ of solvent. Duration: two months. SLT: Sailuotong; APP: amyloid precursor protein; PS1: presenilin-1. One-way analysis of variance was employed to make comparisons among groups, and in the case of the normal distribution, Tukey's post hoc test was conducted; otherwise, the Kruskal–Wallis test was adopted. Compared with C57 sham-operated group, $^{a}P < 0.01$, $^{d}P < 0.05$; compared with APP/PS1 ischemia group, $^{b}P < 0.05$, $^{c}P < 0.01$; compared with C57 ischemia group, $^{e}P < 0.05$.

VEGF and *LRP-1* genes in mouse brain tissue ($P < 0.01$ and $P < 0.05$, respectively) (Table 7).

4. DISCUSSION

This study's behavioural results showed that SLT improved cognitive impairment in APP/PS1 mice. The accumulation of Aβ resulted in a decrease in the learning ability and memory function of the AD mice, which were recovered by the addition of SLT, indicating that it improved the intelligence of the mice with dementia. In addition, SLT can promote vascular proliferation and Aβ clearance by increasing the expression of VEGF and LRP-1, thus improving vascular endothelium and repairing the mitochondrial structure.

The main pathological feature of AD is plaque composed of Aβ peptide. The formation of Aβ plaques results from the amyloidogenic cleavage of human APP.[26] Genetic, biochemical and behavioural research suggests that the physiological generation of the neurotoxic Aβ peptide from sequential APP proteolysis is crucial in the development of AD.[27] Aβ is toxic to neurons in a myriad of ways. It can cause pore formation (resulting in the leakage of ions), a disruption of cellular calcium balance and a loss of membrane potential. It can promote apoptosis, cause synaptic loss and disrupt the cytoskeleton.[26] These reactions can lead to a series of pathological damages, such as the formation of plaques and neurofibrillary tangles, eventually leading to AD.

The behavioural responses of the different mouse groups were tested using a Morris water maze test. The results showed that the number of crossings, swimming times and distances of the APP/PS1 mouse group were worse than those of the ischaemic mouse group. The results of the step-down test showed that the latency of the APP/PS1 mice was higher than in the ischaemic mice, but the number of step-ups was lower than that in the ischemia group. The accumulation of Aβ resulted in decreased learning ability and memory function in the AD mice. The above results all improved when SLT was used, which indicated that it improved intelligence in the mice with dementia.

SLT is a standardised herb preparation containing Renshen (*Radix Ginseng*), Yinxingye (*Folium Ginkgo*) and Honghua (*Flos Carthami*) in three specific doses to treat vascular dementia. These herbal components have been proven to avert or treat circulatory diseases, such as hypertension and stroke. A previous study showed that SLT mediates neuroinflammation, thereby protecting against ischaemic brain injury by inhibiting astrogliosis and suppressing neuroinflammation *via* the LCN2-JAK2/STAT3 pathway.[15] The use of SLT has also been proven effective for the treatment of vascular dementia and has the potential to improve working memory performance in healthy adults.[28, 29]

The concept of NVUs emerged from the first Stroke Progress Review Group meeting of the National Institute of Neurological Disorders and Stroke of the National Institutes of Health (July 2001) to emphasise the unique relationship between brain cells and cerebral vasculature. The NVU was defined as a structure formed by neurons, interneurons, astrocytes and basal lamina covered with smooth muscle cells, pericytes,[30, 31] endothelial cells and an extracellular matrix. Each component is intimately and reciprocally linked to establish an anatomical and functional whole, resulting in a highly efficient cerebral blood flow regulation system. Each component of the NVU plays a specific and active role that maintains dynamic linkages under physiological conditions.[32] In this study, HE staining showed that the number, morphology, arrangement and extracellular space of the neurons in the CA1 hippocampus region of the mice in the APP/PS1 double-transgenic model mouse group were significantly changed. The condition was worse in the APP/PS1 double-transgenic model ischemia group, while SLT restored the pathological changes of the NVUs. Congo red staining revealed that SLT also improved the scattered orange-red sediments in the upper cortex and hippocampus of the APP/PS1 and APP/PS1

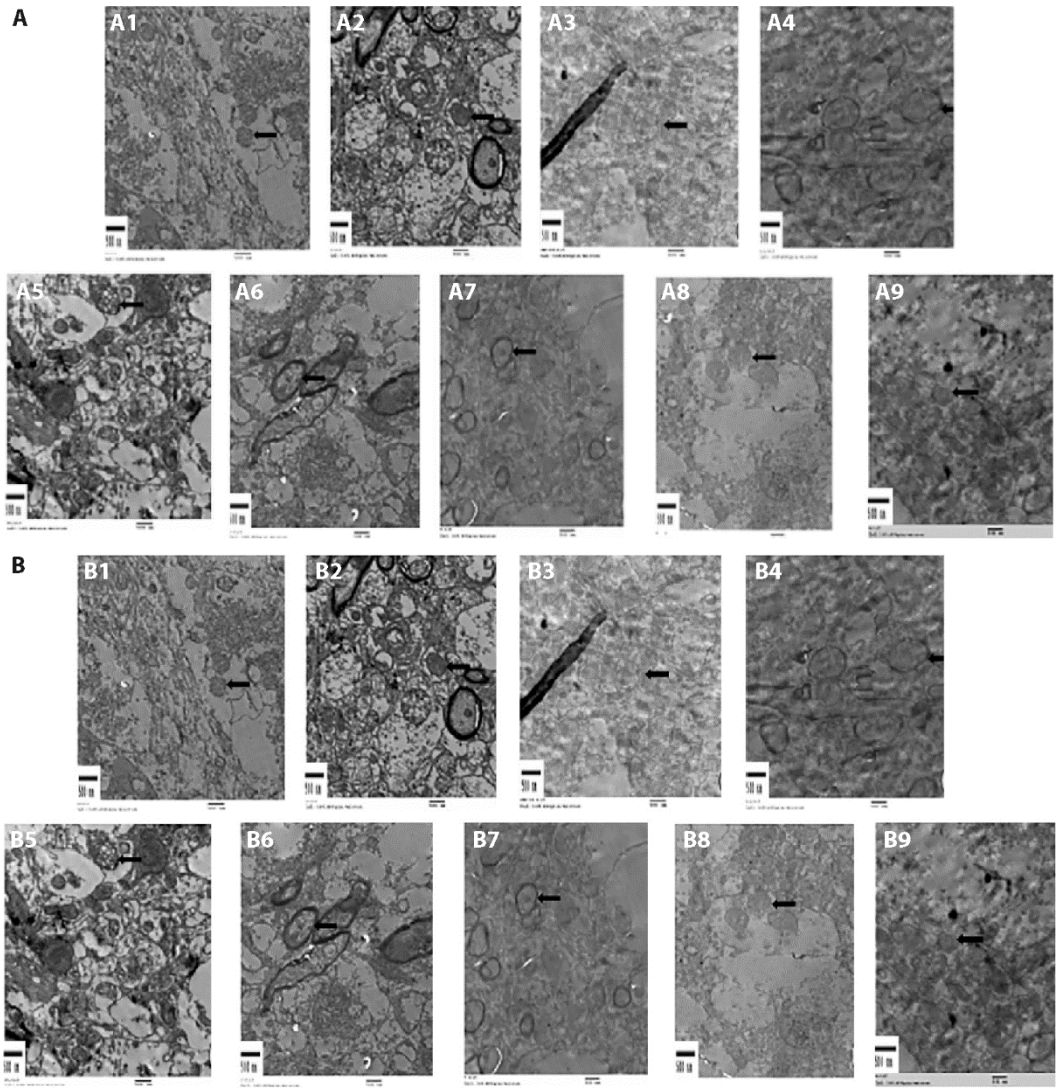

Figure 3 Effect of the method of replenishing *Qi* and activating blood on the ultrastructure of hippocampus and cortical blood vessels in APP/PS1 double transgenic ischemic mice

A: ultrastructure of brain tissue hippocampus; B: ultrastructure of cortical blood vessels. Scale bars = 500 nm. A1/B1: C57 sham-operated group; A2/B2: C57 ischemia group; A3/B3: APP/PS1 model group; A4/B4: APP/PS1 ischemia group; A5/B5: C57BL ischaemic + aspirin group at dose of 20 mg·kg^{-1}·d-1 A6/B6: C57BL ischaemic + SLT group at dose of 32 mg·kg^{-1}·d^{-1}; A7/B7: APP/PS1 + SLT group at dose of 32 mg·kg^{-1}·d^{-1}; A8/B8: APP/PS1 ischaemic + donepezil hydrochloride group at dose of 32 mg·kg^{-1}·d^{-1}; A9/B9: APP/PS1 ischaemic + SLT group at dose of 32 mg·kg^{-1}·d^{-1}. Ischaemic treatment: both right and left common carotid arteries were separated, and the arterial blood vessel was stimulated with a temperature-controlled current of 80 mu A using an *in vivo* thrombometer to cause thrombosis. Duration: two months. SLT: Sailuotong; APP: amyloid precursor protein; PS1: presenilin-1.

ischaemic mice. Both the expression of APP and $A\beta_{1\text{-}42}$ were increased by ischemia but recovered by SLT.

Collateral stasis is a lesion caused by obstruction because of collateral deficiency and urgency, leading to *Qi* and blood stagnation. In the pathological process of cerebral infarction, the occlusion of microvessels induced by a variety of factors leads to cerebral microcirculation disorder and causes cerebral infarction (the TCM pathological mechanism of which still falls into the category of collateral stasis).[14] Therefore, therapies promoting blood circulation and tonify *Qi* are often adopted for treatment, while other syndromes are considered. Modern medical research shows that under normal circumstances, the paracrine function of cerebral microvascular endothelial cells has a significant protective effect on neurons, but this effect is reduced when the endothelial cells are damaged; therefore, the protection and promotion of proliferation of these endothelial cells in cerebral infarction should help improve the central nervous system function.[33]

Furthermore, SLT significantly reduced Aβ content in mice. Ultrastructural observation of NVUs showed that SLT improved the vascular endothelium and repaired the mitochondrial structure. These results indicate that SLT protects the function of the NVUs and promotes both vascular proliferation and Aβ clearance. In turn, it might promote blood circulation and tonify *Qi*.

In order to study the mechanism behind these results, we conducted further experiments. The results of ELISA, western blot and qRT-PCR analysis showed that SLT significantly increased the contents of VEGF, Ang and bFGF, as well as the expression of LRP-1 and VEGF

Table 4 Effect of replenishing *Qi* and activating blood on Aβ protein content in the cerebrospinal fluid in APP/PS1 double transgenic ischemic mice of each group (ng/mL, $\bar{x} \pm s$)

Group	Dose ($mg \cdot kg^{-1} \cdot d^{-1}$)	*n*	Aβ
C57 sham-operated	-	10	0.79±0.25
C57 ischemia	-	10	1.06±0.16
APP/PS1 model	-	10	1.22±0.27[a]
APP/PS1 ischemia	-	10	1.52±0.13[b]
C57BL ischaemic + aspirin	32	10	0.75±0.29
C57BL ischaemic + SLT	32	10	0.79±0.29
APP/PS1 + SLT	32	10	0.75±0.29
APP/PS1 ischaemic + donepezil hydrochloride	20	10	0.82±0.30[c]
APP/PS1 ischaemic + SLT	32	10	0.79±0.26[c]

Notes: ischaemic treatment: both right and left common carotid arteries were separated, and the arterial blood vessel was stimulated with a temperature-controlled current of 80 mu A using an *in vivo* thrombometer to cause thrombosis. The APP/PS1 ischaemic + donepezil hydrochloride group were administered intragastrically with 20 $mg \cdot kg^{-1} \cdot d^{-1}$ of donepezil hydrochloride. The C57BL ischaemic + aspirin group were administered intragastrically with 32 $mg \cdot kg^{-1} \cdot d^{-1}$ of aspirin, the SLT group were administered intragastrically with 32 $mg \cdot kg^{-1} \cdot d^{-1}$ of SLT and the control group were given 32 $mg \cdot kg^{-1} \cdot d^{-1}$ of solvent. Duration: two months. SLT: Sailuotong; APP: amyloid precursor protein; PS1: presenilin-1. One-way analysis of variance was employed to make comparisons among groups, and in the case of the normal distribution, Tukey's post hoc test was conducted; otherwise, the Kruskal–Wallis test was adopted. Compared with C57 sham-operated group, [a]$P < 0.05$, [b]$P < 0.01$; compared with APP/PS1 ischemia group, [c]$P < 0.01$.

Table 5 Effects of supplementing *Qi* and Activating blood circulation on VEGF, Ang, bFGF content in APP/PS1 double transgenic ischemic mice (ng/mg, $\bar{x} \pm s$)

Group	*n*	VEGF	Ang	bFGF
C57 sham-operated	10	9.6±1.2	1.6±0.5	6.4±2.1
C57 ischemia	10	12.4±2.4[a]	1.5±0.2	6.6±0.5
APP/PS1 model	10	6.8±1.7[a]	1.2±0.8	5.8±2.4
APP/PS1 ischemia	10	10.5±3.0	1.4±0.5	5.6±1.6
C57BL ischaemic + aspirin	10	10.4±2.3	1.9±0.6	8.7±2.5
C57BL ischaemic + SLT	10	14.3±1.5[b]	2.9±0.7[b]	9.6±2.5[b]
APP/PS1 + SLT	10	13.6±4.1[c]	1.9±0.7	9.8±1.6
APP/PS1 ischaemic + donepezil hydrochloride	10	10.4±2.0[c]	2.0±0.3[c]	5.8±1.4
APP/PS1 ischaemic + SLT	10	13.7±1.3[c]	2.0±0.4[c]	7.0±1.9[c]

Notes: ischaemic treatment: both right and left common carotid arteries were separated, and the arterial blood vessel was stimulated with a temperature-controlled current of 80 mu A using an *in vivo* thrombometer to cause thrombosis. The APP/PS1 ischaemic + donepezil hydrochloride group were administered intragastrically with 20 $mg \cdot kg^{-1} \cdot d^{-1}$ of donepezil hydrochloride. The C57BL ischaemic + aspirin group were administered intragastrically with 32 $mg \cdot kg^{-1} \cdot d^{-1}$ of aspirin, the SLT group were administered intragastrically with 32 $mg \cdot kg^{-1} \cdot d^{-1}$ of SLT and the control group were given 32 $mg \cdot kg^{-1} \cdot d^{-1}$ of solvent. Duration: two months. SLT: Sailuotong; APP: amyloid precursor protein; PS1: presenilin-1; VEGF: vascular endothelial growth factor; Ang: angiopoietin; bFGF: basic fibroblast growth factor. One-way analysis of variance was employed to make comparisons among groups, and in the case of the normal distribution, Tukey's post hoc test was conducted; otherwise, the Kruskal–Wallis test was adopted. Compared with C57 sham-operated group, [a]$P < 0.05$, compared with C57 ischemia group, [b]$P < 0.05$, compared with APP/PS1 ischemia group, [c]$P < 0.05$.

genes and proteins in brain tissue. These results indicate that SLT can promote blood circulation and tonify *Qi*.

VEGF is a neuroprotective cytokine that promotes neurogenesis and angiogenesis in the brain. Animal models have been used to show that environmental enrichment and exercise (i.e. two non-pharmacological interventions beneficial for postponing the progression of AD and depressive-like behaviour) enhance hippocampal VEGF expression and neurogenesis. In addition, stimulation of VEGF expression promotes neurotransmission and synaptic plasticity processes, such as neurogenesis.[32] Studies have found that VEGF can significantly inhibit the Aβ-induced apoptosis of endothelial cells, and VEGF improves the cognitive impairment of transgenic AD mice.[34] These results indicated that SLT could delay the progression of AD and improve cognitive impairment by inducing angiogenesis and neurogenesis to activate blood circulation and promote tonify *Qi*.

As an Aβ scavenger receptor, LRP-1 is highly expressed in neurons and located on the abluminal side of cerebral capillaries. Its reduced expression in AD patients leads to increased deposition of brain Aβ. Recent evidence revealed that following 1,25-$(OH)_2D_3$ treatment, LRP-1 expression increased significantly in both *in vivo* and *in vitro* studies.[35] Low-density LRP-1 is a member of the low density lipoprotein receptor family and functions as a multifunctional scavenger and signal receptor, as well as a lipoprotein-containing transporter of cholesterol and apolipoprotein E (apoE). Like RAGE, LRP-1 binds a wide range of ligands, including apoE, α2-macroglobulin, APP and Aβ. The transport of Aβ from the bloodstream into the brain is mediated by RAGE, and Aβ transport from the brain into the bloodstream is mediated by LRP-1.[36] Therefore, this study's results may indicate that SLT promotes vascular proliferation by increasing the expression of VEGF and LRP-1.

In conclusion, SLT treatment promotes the proliferation of blood vessels by increasing the expression of VEGF. At the same time, SLT promotes the expression of LRP-1, increases the clearance of Aβ and improves the learning ability and memory function of APP/PS1 mice.

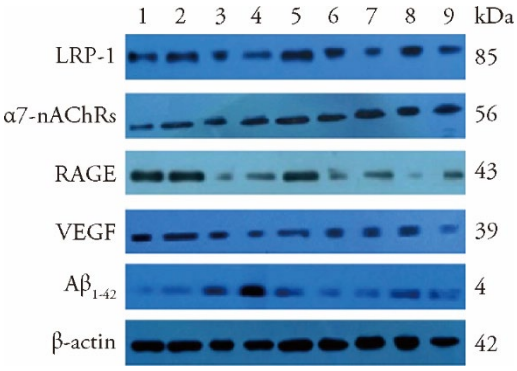

Figure 4 Effect of replenishing *Qi* and activating blood on the expression of related proteins in APP/PS1 ischemia model mice ($\bar{x} \pm s$, n = 10)

1: C57 sham-operated group; 2: C57 ischemia group; 3: APP/PS1 model group; 4: APP/PS1 ischemia group; 5: C57BL ischaemic + aspirin group at dose of 20 mg·kg^{-1}·d^{-1}; 6: C57BL ischaemic + SLT group at dose of 32 mg·kg^{-1}·d^{-1}; 7: APP/PS1 + SLT group at dose of 32 mg·kg^{-1}·d^{-1}; 8: APP/PS1 ischaemic + donepezil hydrochloride group at dose of 32 mg·kg^{-1}·d^{-1}; 9: APP/PS1 ischaemic + SLT group at dose of 32 mg·kg^{-1}·d^{-1}. Ischaemic treatment: both right and left common carotid arteries were separated, and the arterial blood vessel was stimulated with a temperature-controlled current of 80 mu A using an *in vivo* thrombometer to cause thrombosis. Duration: two months. SLT: Sailuotong; APP: amyloid precursor protein; PS1: presenilin-1.

These results confirm that SLT protects the function of new blood vessels by promoting vascular proliferation and Aβ clearance.

5. REFERENCES

1. Tripathi SM, Murray AD. Alzheimer's dementia: the emerging role of positron emission tomography. Neuroscientist 2022; 28: 507-19.
2. Scheltens P, De Strooper B, Kivipelto M, et al. Alzheimer's disease. Lancet 2021; 397: 1577-90.
3. Button EB, Robert J, Caffrey TM, et al. Hdl from an Alzheimer's disease perspective. Curr Opin Lipidol 2019; 30: 224-34.
4. Lane CA, Hardy J, Schott JM. Alzheimer's disease. Eur J Neurol 2018; 25: 59-70.
5. Fan L, Mao C, Hu X, et al. New insights into the pathogenesis of Alzheimer's disease. Front Neurol 2019; 10: 1312.
6. Jean L, Foley AC, Vaux DJT. The physiological and pathological implications of the formation of hydrogels, with a specific focus on amyloid polypeptides. Biomolecules 2017; 7: 70.
7. Dauberman WN, Xu S. Alzheimer's disease pathogenesis: the denied access model. OMICS International 2017; 7: 1-10.
8. Kocahan S, Doğan Z. Mechanisms of Alzheimer's disease pathogenesis and prevention: The brain, neural pathology, n-methyl-d-aspartate receptors, tau protein and other risk factors. Clin Psychopharmacol Neurosci 2017; 15: 1-8.
9. Carvey PM, Hendey B, Monahan AJ. The blood-brain barrier in neurodegenerative disease: a rhetorical perspective. J Neurochem 2009; 111: 291-314.
10. Zlokovic BV. Neurovascular pathways to neurodegeneration in Alzheimer's disease and other disorders. Nat Rev Neurosci 2011; 12: 723-38.
11. Ouellette J, Lacoste B. From neurodevelopmental to neurodegenerative disorders: the vascular continuum. Front Aging Neurosci 2021; 13: 749026.
12. Chen CL, Young SH, Gan HH, et al. Chinese medicine neuroaid efficacy on stroke recovery: a double-blind, placebo-controlled, randomized study. Stroke 2013; 44: 2093-100.
13. Wu B, Liu M, Liu H, et al. Meta-analysis of traditional chinese patent medicine for ischemic stroke. Stroke 2007; 38: 1973-9.
14. Yao W, Yang H, Ding G. Mechanisms of Qi-blood circulation and *Qi* deficiency syndrome in view of blood and interstitial fluid circulation. J Tradit Chin Med 2013; 33: 538-44.
15. Zhang Y, Liu J, Yao M, et al. Sailuotong capsule prevents the cerebral ischaemia-induced neuroinflammation and impairment of recognition memory through inhibition of lcn2 expression. Oxid Med Cell Longev 2019; 2019: 8416105.
16. Shi L, Zheng C, Shen Y, et al. Optical imaging of metabolic dynamics in animals. Nat Commun 2018; 9: 2995.
17. Obafemi TO, Owolabi OV, Omiyale BO, et al. Combination of donepezil and gallic acid improves antioxidant status and cholinesterases activity in aluminum chloride-induced neurotoxicity in wistar rats. Metab Brain Dis 2021; 36: 2511-9.
18. Lian W, Jia H, Xu L, et al. Multi-protection of dl0410 in ameliorating cognitive defects in d-galactose induced aging mice. Front Aging Neurosci 2017; 9: 409.
19. Chung CY, Licznerski P, Alavian KN, et al. The transcription factor orthodenticle homeobox 2 influences axonal projections and vulnerability of midbrain dopaminergic neurons. Brain 2010;

Table 6 Effect of replenishing *Qi* and activating blood on VEGF, Aβ$_{1-42}$, α7-nAChRs, RAGE and LRP-1 protein content in the brain tissues in APP/PS1 double transgenic ischemic mice of each group ($\bar{x} \pm s$)

Group	n	VEGF	Aβ$_{1-42}$	α7-nAChRs	RAGE	LRP-1
C57 sham-operated	10	1.000±0.172	1.000±0.073	1.000±0.131	1.000±0.074	1.000±0.203
C57 ischemia	10	1.710±0.088^{a}	0.930±0.122	1.410±0.153^{a}	1.052±0.091	0.970±0.072
APP/PS1 model	10	0.620±0.045^{a}	1.550±0.124^{d}	1.560±0.065^{a}	1.150±0.116	0.800±0.103
APP/PS1 ischemia	10	0.500±0.046^{a}	2.730±0.270^{a}	2.250±0.083^{a}	1.518±0.077^{a}	0.600±0.054^{d}
C57BL ischaemic + aspirin	10	1.330±0.022^{b}	1.040±0.111	1.380±0.142	1.050±0.062	1.160±0.104 ^{f}
C57BL ischaemic + SLT	10	1.880±0.042	0.960±0.115	1.110±0.144	1.010±0.052	1.050±0.200
APP/PS1 + SLT	10	1.040±0.081^{c}	1.200±0.132^{c}	1.160±0.120^{c}	1.020±0.079^{c}	1.260±0.064^{c}
APP/PS1 ischaemic + donepezil hydrochloride	10	0.580±0.084	1.560±0.127^{c}	1.250±0.256^{c}	1.230±0.075^{e}	1.180±0.085^{c}
APP/PS1 ischaemic + SLT	10	0.839±0.095^{c}	1.460±0.273^{c}	1.480±0.135^{ac}	1.240±0.151^{ac}	1.220±0.032^{c}

Notes: ischaemic treatment: both right and left common carotid arteries were separated, and the arterial blood vessel was stimulated with a temperature-controlled current of 80 mu A using an *in vivo* thrombometer to cause thrombosis. The APP/PS1 ischaemic + donepezil hydrochloride group were administered intragastrically with 20 mg·kg^{-1}·d^{-1} of donepezil hydrochloride. The C57BL ischaemic + aspirin group were administered intragastrically with 32 mg·kg^{-1}·d^{-1} of aspirin, the SLT group were administered intragastrically with 32 mg·kg^{-1}·d^{-1} of SLT and the control group were given 32 mg·kg^{-1}·d^{-1} of solvent. Duration: two months. SLT: Sailuotong; APP: amyloid precursor protein; PS1: presenilin-1; VEGF: vascular endothelial growth factor; Aβ$_{1-42}$: amyloid-beta1-42; α7-nAChRs: α7-nicotinic acetylcholine receptor; RAGE: anti-receptor for advanced glycation endproducts; LRP-1: lipoprotein receptor-related-protein-1. One-way analysis of variance was employed to make comparisons among groups, and in the case of the normal distribution, Tukey's post hoc test was conducted; otherwise, the Kruskal–Wallis test was adopted. Compared with C57 sham-operated group, ^{a}P <0.01, ^{d}P < 0.05; compared with C57 ischemia group, ^{b}P < 0.01, ^{f}P < 0.05; compared with APP/PS1 ischemia group, ^{c}P < 0.01, ^{e}P < 0.05.

Table 7 Effect of replenishing *Qi* and activating blood on mRNA expressions of VEGF, APP, α7-nAChRs, RAGE and LRP-1 in APP/PS1 double transgenic ischemic mice of each group ($\bar{x} \pm s$)

Group	*n*	VEGF	APP	α7-nAChRs	RAGE	LRP-1
C57 sham-operated	10	0.800±0.150	0.720±0.392	1.200±0.291	1.090±0.392	1.160±0.713
C57 ischemia	10	1.450±0.730[a]	0.680±5.254	1.120±3.022	0.730±2.991	1.570±0.959[a]
APP/PS1 model	10	0.180±0.080[a]	1.070±0.045[a]	0.190±0.040[a]	2.090±0.031[a]	0.380±0.191[a]
APP/PS1 ischemia	10	0.540±0.481[a]	2.730±1.132[a]	0.320±0.903[a]	2.670±0.675[a]	0.850±1.052[a]
C57BL ischaemic + aspirin	10	0.860±0.421[b]	0.680±5.250	0.400±0.212[d]	0.480±0.214[b]	1.380±2.053[b]
C57BL ischaemic + SLT	10	1.490±0.111	0.150±0.190[d]	0.320±0.192[d]	0.110±0.091[d]	1.250±0.312[c]
APP/PS1 + SLT	10	0.630±0.450[c]	0.580±0.626	0.700±0.580	0.501±0.455	1.680±0.523[c]
APP/PS1 ischaemic + donepezil	10	0.160±0.121	0.420±0.480	0.630±0.002	1.240±0.244	1.490±0.422[c]
APP/PS1 ischaemic + SLT	10	0.930±0.345[c]	0.690±0.242	1.180±1.591	2.090±0.915	1.420±0.560[c]

Notes: ischaemic treatment: both right and left common carotid arteries were separated, and the arterial blood vessel was stimulated with a temperature-controlled current of 80 mu A using an *in vivo* thrombometer to cause thrombosis. The APP/PS1 ischaemic + donepezil hydrochloride group were administered intragastrically with 20 $mg \cdot kg^{-1} \cdot d^{-1}$ of donepezil hydrochloride. The C57BL ischaemic + aspirin group were administered intragastrically with 32 $mg \cdot kg^{-1} \cdot d^{-1}$ of aspirin, the SLT group were administered intragastrically with 32 $mg \cdot kg^{-1} \cdot d^{-1}$ of SLT and the control group were given 32 $mg \cdot kg^{-1} \cdot d^{-1}$ of solvent. Duration: two months. SLT: Sailuotong; APP: amyloid precursor protein; PS1: presenilin-; VEGF: vascular endothelial growth factor; α7-nAChRs: α7-nicotinic acetylcholine receptor; RAGE: anti-receptor for advanced glycation endproducts; LRP-1: lipoprotein receptor-related-protein-1. One-way analysis of variance was employed to make comparisons among groups, and in the case of the normal distribution, Tukey's post hoc test was conducted; otherwise, the Kruskal–Wallis test was adopted. Compared with C57 sham-operated group, [a]$P < 0.05$; compared with C57 ischemia group, [b]$P < 0.05$, [d]$P < 0.01$; compared with APP/PS1 ischemia group, [c]$P < 0.05$, [c]$P < 0.01$.

133: 2022-31.
20. Li P, Lu M, Shi J, et al. Lung mesenchymal cells elicit lipid storage in neutrophils that fuel breast cancer lung metastasis. Nat Immunol 2020; 21: 1444-55.
21. Wang J, Sun BL, Xiang Y, et al. Capsaicin consumption reduces brain amyloid-beta generation and attenuates Alzheimer's disease-type pathology and cognitive deficits in app/ps1 mice. Transl Psychiatry 2020; 10: 230.
22. Wang Z, Liu CY, Zhao Y, Dean J. Figla, lhx8 and sohlh1 transcription factor networks regulate mouse oocyte growth and differentiation. Nucleic Acids Res 2020; 48: 3525-41.
23. Kou J, Yang J, Lim JE, et al. Catalytic immunoglobulin gene delivery in a mouse model of Alzheimer's disease: prophylactic and therapeutic applications. Mol Neurobiol 2015; 51: 43-56.
24. Kaczmarczyk A, Hempel AM, Von Arx C, et al. Precise timing of transcription by c-di-gmp coordinates cell cycle and morphogenesis in caulobacter. Nat Commun 2020; 11: 816.
25. Guttenplan KA, Weigel MK, Adler DI, et al. Knockout of reactive astrocyte activating factors slows disease progression in an als mouse model. Nat Commun 2020; 11: 3753.
26. Reiss AB, Arain HA, Stecker MM, Siegart NM, Kasselman LJ. Amyloid toxicity in Alzheimer's disease. Rev Neurosci 2018; 29: 613-27.
27. O'brien RJ,Wong PC. Amyloid precursor protein processing and Alzheimer's disease. Annu Rev Neurosci 2011; 34: 185-204.
28. Jia J, Wei C, Chen S, et al. Efficacy and safety of the compound chinese medicine sailuotong in vascular dementia: a randomized clinical trial. Alzheimers Dement (N Y) 2018; 4: 108-17.
29. Steiner GZ, Yeung A, Liu JX, et al. The effect of sailuotong (slt) on neurocognitive and cardiovascular function in healthy adults: a randomised, double-blind, placebo controlled crossover pilot trial. BMC Complement Altern Med 2016; 16: 15.
30. Vickrey BG, Brott TG, Koroshetz WJ. Research priority setting: a summary of the 2012 ninds stroke planning meeting report. Stroke 2013; 44: 2338-42.
31. Iadecola C. The neurovascular unit coming of age: a journey through neurovascular coupling in health and disease. Neuron 2017; 96: 17-42.
32. Echeverria V, Barreto GE, Avila-Rodriguezc M, Tarasov VV, Aliev G. Is vegf a key target of cotinine and other potential therapies against alzheimer disease? Curr Alzheimer Res 2017; 14: 1155-63.
33. Li W, Li P, Hua Q, et al. The impact of paracrine signaling in brain microvascular endothelial cells on the survival of neurons. Brain Res 2009; 1287: 28-38.
34. Religa P, Cao R, Religa D, et al. Vegf significantly restores impaired memory behavior in Alzheimer's mice by improvement of vascular survival. Sci Rep 2013; 3: 2053.
35. Patel P, Shah J. Role of vitamin d in amyloid clearance *via* lrp-1 upregulation in Alzheimer's disease: a potential therapeutic target? J Chem Neuroanat 2017; 85: 36-42.
36. Donahue JE, Flaherty SL, Johanson CE, et al. Rage, lrp-1, and amyloid-beta protein in Alzheimer's disease. Acta Neuropathol 2006; 112: 405-15.